

BACKGROUND

STAT proteins Signal transducer and activator of transcription (STAT) proteins are a pleiotropic family of transcription factors controlling cellular functions in various cell types. There are seven STAT proteins in humans: STAT1, STAT2, STAT3, STAT4, STAT5a, STAT5b, and STAT6. STAT proteins enable cellular responses to external stimuli by communicating between transmembrane receptors and the nucleus. Cytokines binding induces phosphorylation by Janus kinases (JAKs), which in turn phosphorylate STAT proteins. pSTATs then form hetero- or homodimers, translocate into the nucleus, and initiate gene transcription programs. STAT proteins are broadly involved in immune responses, including regulating immune cell proliferation, polarization, and memory formation. pSTATs have shown to be of interest in cancer outcomes and may have therapeutic implications.

Rationale:

Interrogating of all known STAT proteins simultaneously at single cell resolution is rarely performed. Further, it is rare for more than one residue to be assessed for a single STAT protein, despite phosphorylation of different residues conferring unique signaling and translocation characteristics. Flow cytometry allows acquisition of multi-dimensional data at single cell resolution, relatively cheaply and rapidly, overcoming many of the limitations of traditional western blots.

METHODS

We developed a flow cytometry panel to assess tyrosine phosphorylation of six STAT proteins (STAT1, STAT2, STAT3, STAT4, STAT5a, STAT6) and additional serine residue phosphorylations on STAT1 and STAT3. Panels were optimized for fixation method, antibody clones and antibodies titrations. FlowJo software was used for data acquisition and analysis, with statistical analyses performed in R.

PANEL DESIGN

Vendor	Catalogue	Host	Target	Clone	Antigen	Fluorochrome
BioLegend	686412	Mouse	Human	A15158B	Stat1(p727)	AF647
BDBiosciences	562985	Mouse	Human	4a	Stat1 (pY701)	BV421
R&D	IC2890N	Rabbit	Human	1021D	Stat2 (Y689)	AF700
BDBiosciences	558557	Mouse	Human	49/p-Stat3	Stat3 (pS727)	PE
BDBiosciences	562673	Mouse	Human	4/P-STAT3	Stat3 (pY705)	PE-CF594
BDBiosciences	558136	Mouse	Human	38/p-Stat4	STAT4 (pY693)	AF488
BDBiosciences	560117	Mouse	Human	47/Stat5(pY694)	Stat5 (pY694)	PECY7
BDBiosciences	561195	Mouse	Human	18/P-Stat6	Stat6 (pY641)	PerCPyC5.5

Gating Strategy

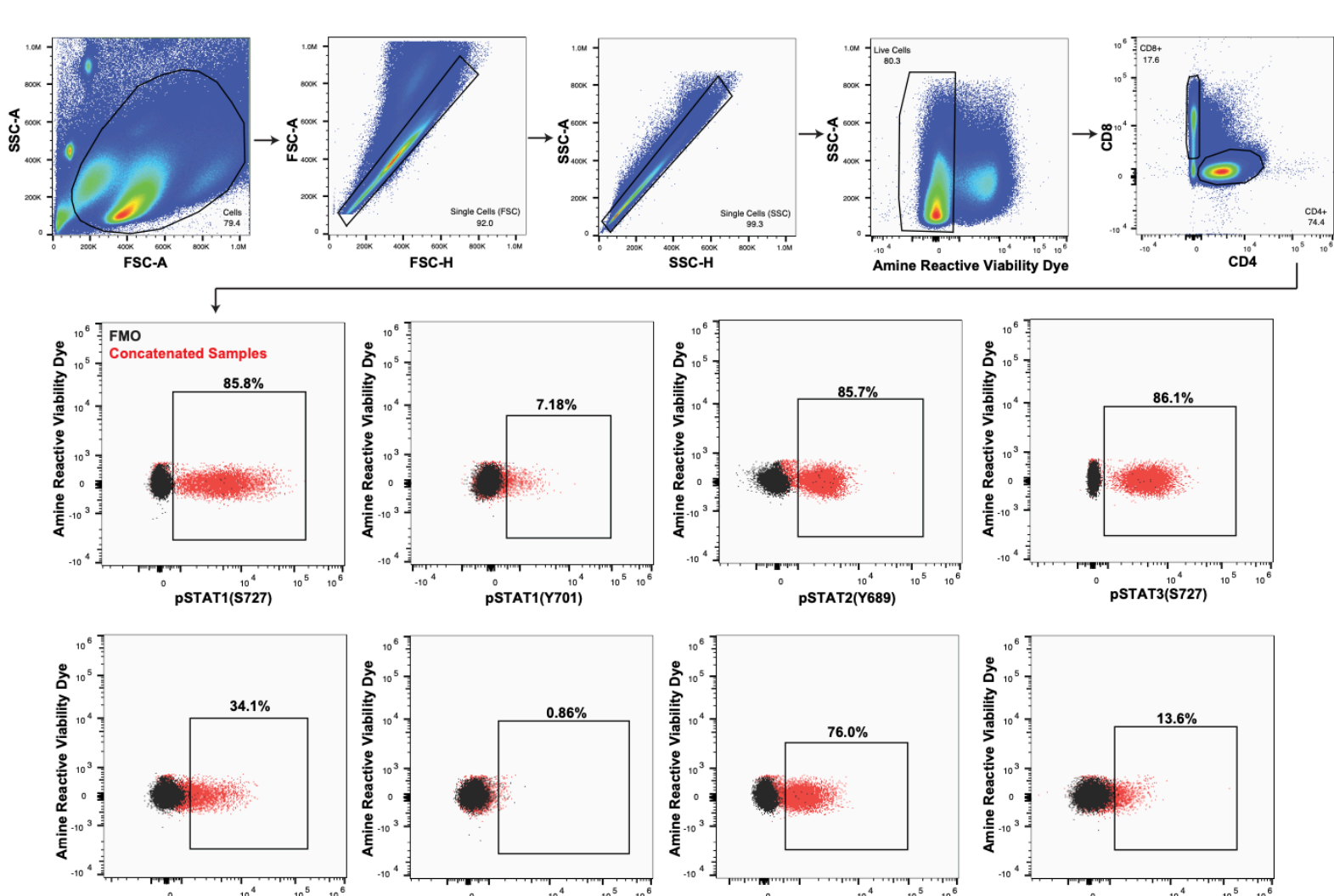


Figure 1. T-cells were assessed for the panel's markers. The resulting fcs files concatenated. Debris and doublets were excluded. Viable cells were gated based on absence of the amine reactive viability dye Live Dead Near IR, then gated into CD4+ and CD8+ populations. Expression of each pSTAT protein is shown in red and the corresponding FMO in black. Frequencies of positive cells are shown above the corresponding gate.

RESULTS

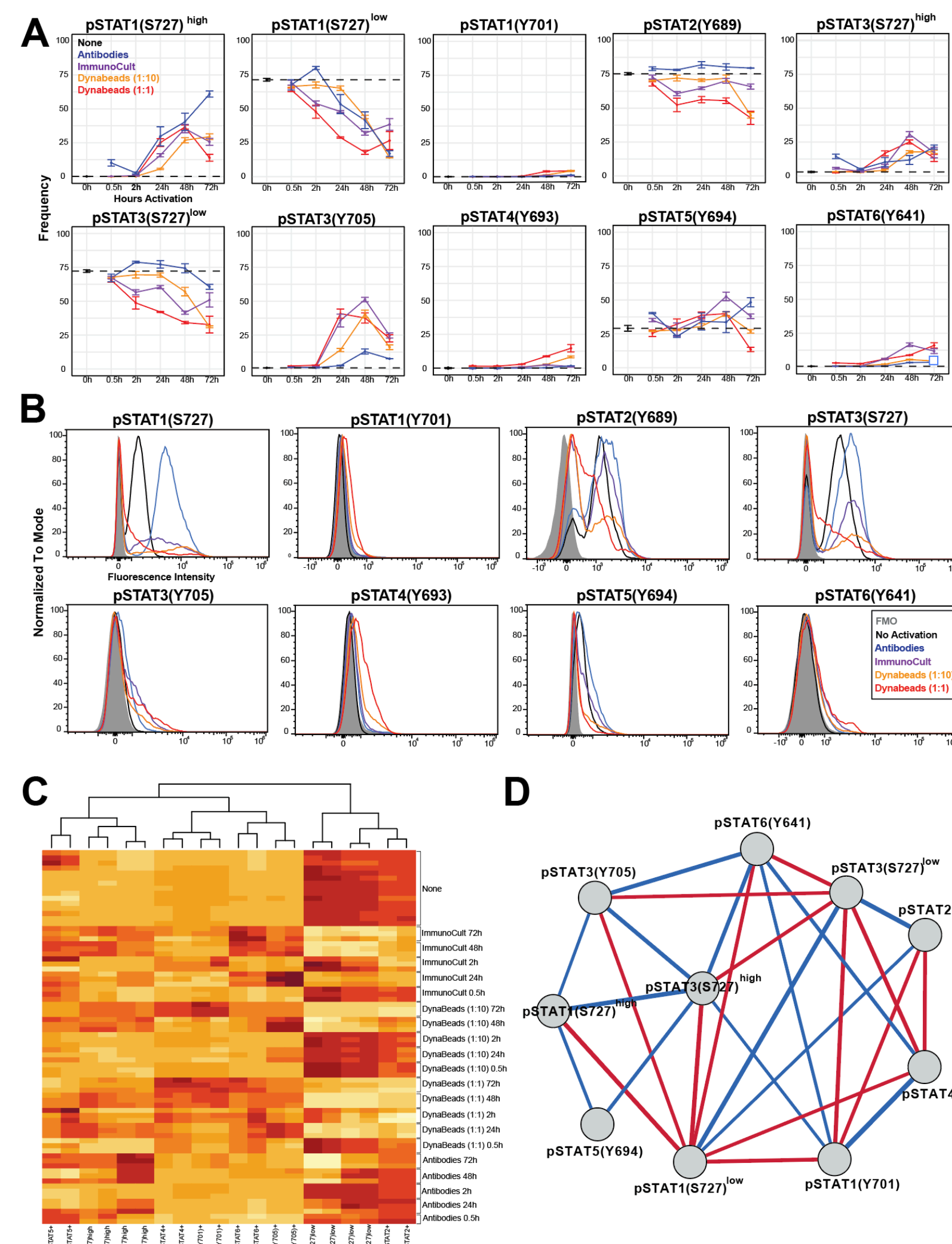


Figure 2. T-cell activation via CD3/CD28 stimulation enhances expression of all pSTATs. We initially tested our panel to assess the impact of polyclonal T-cell activation on the expression of pSTATs. Cells were left unstimulated (0h timepoint) or activated for times indicated.

(A) At baseline (no activation), high frequencies of pSTAT1(S727), pSTAT2(Y689) and pSTAT3(S727) expressing T-cells were observed. Two positivity states, "low" and "high" were observed in some residues. pSTAT1(S727)^{low} and pSTAT3(S727)^{low} frequencies were elevated at baseline, but the "high" states were absent. Increases in pSTAT1(S727)^{high}, pSTAT1(Y701), pSTAT3(S727)^{high}, pSTAT3(Y705), pSTAT4(Y693) and pSTAT6(Y641) occurred at the 24 hour timepoint. Only minor, inconsistent changes were observed in pSTAT5(Y694) expression. Error bars show the standard error of the mean (SEM).

(B) Representative histograms of pSTAT residue expression in CD4+ T-cells at the 72-hour timepoint are shown. Corresponding FMO samples are shown in shaded grey and and late bound CD3 with soluble CD28 antibodies in blue.

(C) A heatmap of frequencies of pSTAT+ CD4+ and CD8+ T-cells is shown. Column data (pSTATs) were scaled and centered and ordered/grouped based on hierarchical clustering using Euclidean distance.

(D) Frequencies of pSTAT+ CD4+ T-cells were assessed for correlations and visualized as a network, with positive correlations in blue and negative correlations in red.

Figure 3. Assessment of pSTAT induction by recombinant cytokines.

(A) T-cells were isolated via negative CD3+ selection and cultured for the indicated amounts of time with three concentrations of IFN β . Error bars show the SEM. Increases in pSTAT1(Y701), pSTAT3(Y705) and pSTAT4(Y693) frequency were observed as early as the 15-minute timepoint, with negligible differences at different concentrations of IFN β . No changes occurred in pSTAT2(Y689) frequency. In some timepoints, IFN β decreased pSTAT1(S727)^{high} and pSTAT3(S727)^{high} frequencies while increasing pSTAT1(S727)^{low} and pSTAT3(S727)^{low} in a dose-dependent manner. Though there was low absolute frequency of pSTAT6 positive cells, IFN β stimulation increased in an inverse dose-dependent manner.

(B) T-cells were isolated and cultured with recombinant cytokines for 30 minutes. Frequencies of positive CD4+ T-cells for each pSTAT are shown. Bonferroni corrected t-tests determined significance. Error bars show the SEM. IFN α increased the frequency of all pSTATs except pSTAT1(S727)^{low} and pSTAT3(S727)^{low}. IFN α increased the frequency of these pSTATs, except for pSTAT6(Y641). Canonical associations were also observed including: IL-6/IL-10/IL-15 induction of pSTAT3(Y705), IL-2/IL-7/IL-15 induction of pSTAT5(Y694) and IL-4 induction of pSTAT6(Y641). Interestingly, IL-6 significantly increased the frequencies of pSTAT1(Y701), pSTAT3(Y705), pSTAT6(Y641) and trended towards increases in pSTAT3(S727)^{high} and pSTAT4(Y693).

(C) A heatmap of frequencies of pSTAT+ CD4+ and CD8+ T-cells.

(D) Frequencies were assessed for correlations and visualized as a network

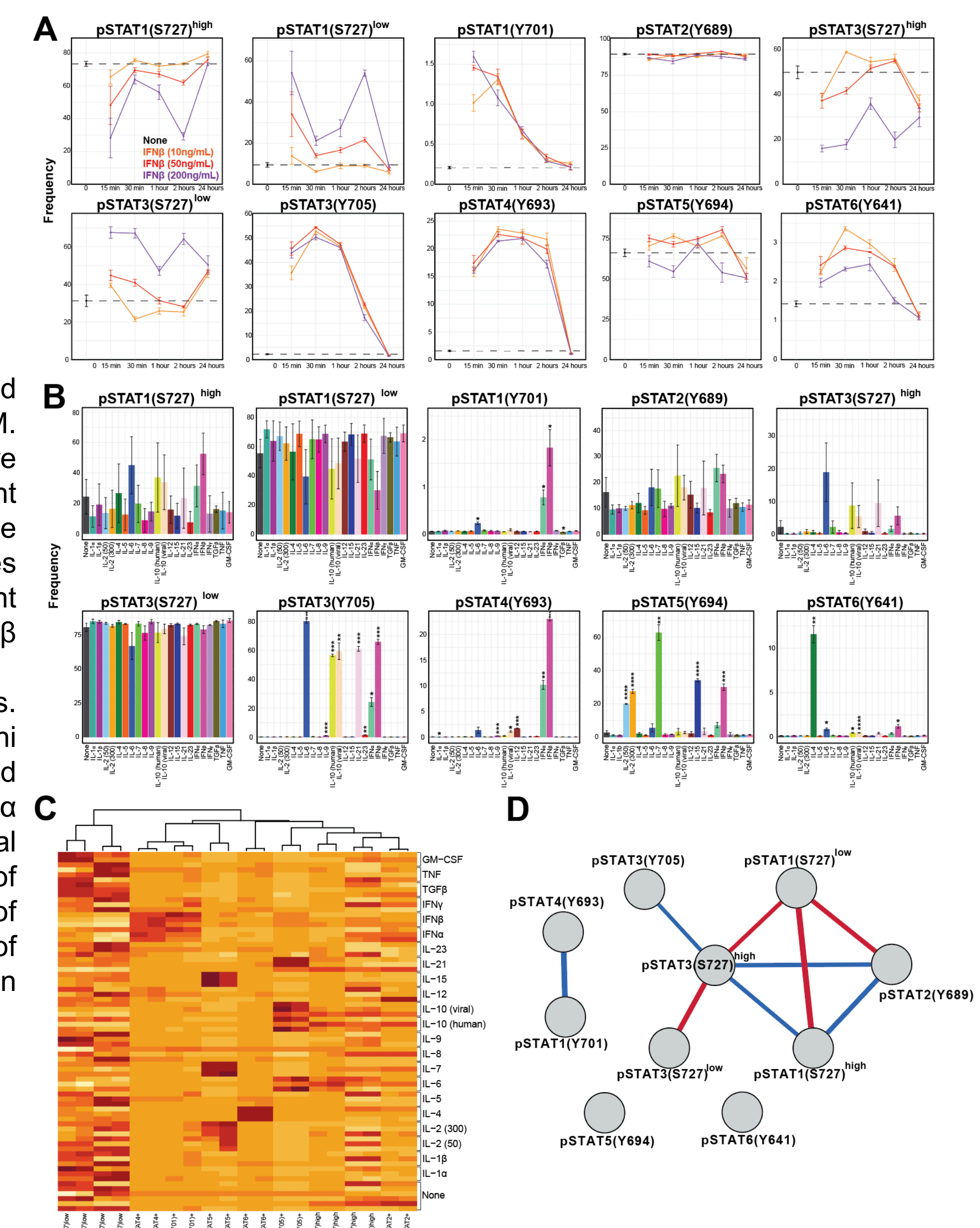
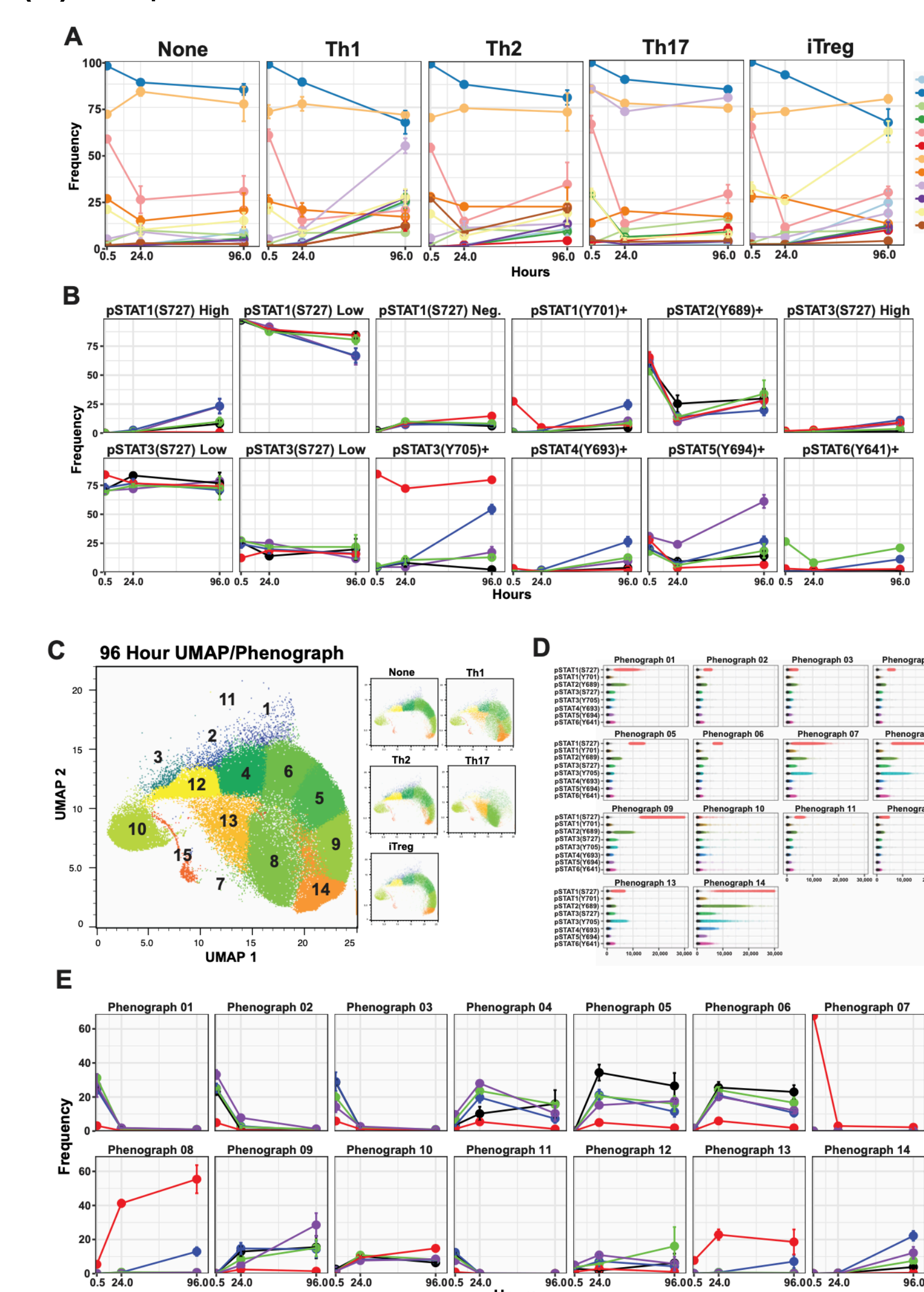


Figure 4. In vitro polarization of naive CD4+ T-cells results in complex pSTAT expression profiles. Naive CD4+ T-cells were isolated and polarized.

(A) Expression of pSTATs in different polarization groups at each time point.

(B) Polarization frequencies for each pSTAT at different time points. Frequencies of canonically associated pSTATs were upregulated in polarized cells: pSTAT1(Y701) in Th1, pSTAT6(Y641) in Th2, pSTAT3(Y705) in Th17, and pSTAT5(Y694) in iTregs. Th1 and iTregs also had increases in pSTAT1(S727)^{high} expression; Th1 also had increases in pSTAT3(Y705) and pSTAT4(Y649) frequencies

(C) The eight pSTAT parameters were reduced to two dimensions by UMAP and assessed for clusters by Phenograph. The concatenated UMAP of the 96-hour timepoints is shown in the large panel, with the Phenograph clusters labeled by number. The 96-hour UMAPs of each polarization group are shown in the smaller panels. At 96 hours, clustering for Th1 and Th17 cells were distinct, but Th2 and iTregs were similar to the unpolarized "None" group

(D) The expression profiles for each pSTAT in each of the Phenograph clusters is plotted. Each cell belonging to the corresponding Phenograph cluster is plotted with its value on the x-axis representing the MFI value for the corresponding y-axis parameter. The MFI values for the corresponding FMO for each pSTAT are shown as black dots.

(E) The frequencies of the polarization groups in each Phenograph cluster are plotted. Results shown are representative of two independent experiments.

CONCLUSIONS

Findings:

- We interrogated the impact of activation, cytokine stimulation and polarization on T-cell pSTAT signaling and noted novel findings.
- pSTAT2(Y689) is constitutively expressed in most T-cells, irrespective of activation or stimulation.
- IFN β and, to a lesser degree, IFN α , rapidly increased the frequency of expression of all pSTATs.
- Both pSTAT1(S727) and pSTAT3(S727) were expressed in most T-cells.
- We defined two positivity states for each of these markers, "low" and "high".
- Activation and specific cytokine stimulation caused shifts between the low to high population.
- In contrast, pSTAT1(Y701) and pSTAT3(Y705) were absent in resting cells, suggesting that phosphorylation of serine and the tyrosine residues have distinct roles in T-cell biology.

Limitations:

- Due to the lack of commercially available antibodies, we did not investigate phosphorylation of serine residues in other STAT molecules.
- We anticipate that as higher dimension flow cytometry becomes increasingly common and additional antibodies are made available, future refinement of this panel will be able to incorporate additional phosphorylated residues.
- We hypothesize that formation of homo- and heterodimers and competition between these different pSTAT complexes add another layer of complexity that also needs to be assessed in studies of pSTAT signaling.
- Though we did not test it in the present study, this panel is theoretically compatible with imaging cytometry, which would allow for assessing dimerization by co-localization, as well as cellular location (i.e. cytoplasmic or nuclear).

Conclusions:

- The results of this study highlight that the often-used model of one pSTAT induced by cytokine stimulation (e.g. IL-10 induction of pSTAT3) or associated with T-cell polarization (e.g. pSTAT5 in Tregs) is oversimplified.
- Optimized for a 96-well format, making it relatively rapid and compatible with medium throughput assays.
- Presently used to interrogate T-cell biology in this study, but is readily compatible with all human cell types.
- Potentially a powerful tool in interrogating the roles of STAT signaling in health and disease.

SUPPORTING INFORMATION

Financial support: R00CA230201

Code for all analyses can be found on our publicly available GitHub.

Emily.monk@cuanschutz.edu